Measurement of Radio Signal Propagation through Window Panes and Energy Saving Windows

Per Ängskog[1,2], Mats Bäckström[1,3], Bengt Vallhagen[3]

[1]Electromagnetic Engineering Lab, KTH Royal Institute of Technology, Stockholm, Sweden, pangskog@kth.se
[2]Department of Electronics, Mathematics, and Natural Sciences, University of Gävle, Gävle, Sweden
[3]Saab Aeronautics, SAAB AB, Linköping, Sweden

***Abstract*—Glass windows have undergone an energy saving evolution over the past three, four decades, from single panes till today's ultralow-emission windows. While the earliest energy saving windows were constructed as a sandwich of clear glass panes using the vacuum-flask principle, modern low-emission windows includes panes with coatings of metal and/or metal oxides. This coating has caused radio propagation problems for communication systems; something that may be utilized to protect a building from intentional electromagnetic interference (IEMI) attacks and to help protecting against information leakage. In this paper measurements of the shielding performance of different generations of windows and qualities of window panes are presented. The intention is to include the results in a guide-line for IEMI protection of critical infrastructures. Measurements are made using two complementary methods; in a nested reverberation chamber and in a semi-anechoic chamber, both over the range 1 – 18 GHz. The results show a clear generation dependency where the energy saving windows largely do not attenuate RF signals at all and low-emission windows offer shielding effectiveness values between 10 and 45 dB with potentially as much as around 60 dB in the upper half of the spectrum.**

Keywords—Intentional EMI; signal propagation; shielding; transmission; glass; energy saving window; low-e window; reverberation chamber;

I. INTRODUCTION

Intentional EMI has become a reality over the last decades at the same time as our society has become increasingly dependent of electrical and electronic systems. Of special concern are the parts of society, that form infrastructures critical for its functionality, such as telecommunications; electric power supply; food and water supply; transportation; and financial institutions including banks and ATM's. Even though it is of special importance that the automation and control of these infrastructures is robust against electromagnetic attacks they are strikingly often based on commercial-of-the-shelf (COTS) equipment fulfilling no more than basic civil EMC specifications. Hence the need for protection against IEMI has grown radically [1], [2], [3].

Today there are several projects in Europe both international and national, working in the field of protecting infrastructures against IEMI [4]. The shielding of buildings is one among several different protective actions available. Traditionally the windows have been considered as one of the weakest points together with physical apertures in form of ventilation openings and similar. However, today this is not necessarily the case regarding windows.

Window panes have undergone a tremendous evolution with respect to maintaining a pleasant indoor climate for homes, offices and commercial buildings. With various types of coatings they can thermally insulate a building; in cold climates preventing the heat from leaking out and in hot climates preventing the heat from entering through the windows. While heat is in the form of infra-red, long wavelength, other glasses have coatings that prevent the high energy, short wavelength, ultra-violet part of the sunlight from entering the building. By combining these glasses into window units a variety of energy saving windows can be constructed.

A large number of different types of coatings have appeared on the market during the last decades which combined creates distinguishable generations of windows. Previous measurements have shown that modern energy efficient windows can have higher attenuation than the walls of the building on frequencies well below the visible spectrum [5]. Several reports have been published about wireless communication systems with degraded performance or even loss of communication at least to some degree due to window installations [6], [7], [8], [9].

This radio attenuation can be taken advantage of in IEMI protection. The measurements presented in this paper are intended for inclusion in an IEMI protection guideline, for critical infrastructures which is being developed for the Swedish Fortifications Agency. There are also benefits to be gained in the other direction, in terms of less information leakage (TEMPEST), due to the reduced electromagnetic radiation out from buildings.

With the purpose to classify window shielding effectiveness (*SE*) this paper examines single window panes and window units of different generations.

II. METHOD

Two different methods were employed to determine the shielding properties of the coated glass structures. The first was a traditional comparative "hatch on/hatch off" measurement under normal incidence plane wave conditions in a semi-anechoic chamber (SAC) environment and the second was a measurement of the isotropic transmission cross section of the

test object with a mode stirred incident field in a nested reverberation chamber (RC).

A. Plane Wave Shielding Effectiveness

The plane wave shielding effectiveness was determined from a comparative measurement, "hatch on/hatch off", measured at normal incidence using two polarizations; see Fig. 1 and Fig. 2. The plane wave shielding effectiveness of the test aperture, $SE_{\text{apert,pw}}$, is given by:

$$SE_{\text{apert,pw}} = \frac{P_{trans,ref}}{P_{trans,apert}} \tag{1}$$

where $P_{\text{trans,ref}}$ denotes the power received in the reference case and $P_{\text{trans,apert}}$ denotes the power received when the glass sample is mounted on the test panel.

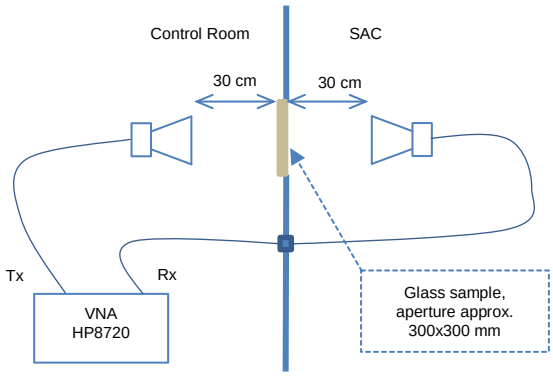

Fig. 1. Block diagram showing the plane wave measurement set-up

The transmitting and receiving antennas were positioned at a 300 mm distance from the sample on the respective side. The size of the test aperture was 300 by 300 mm. For the metal coated samples the metallic coating was in electrical contact with the metal frame of the opening. The frequency interval 1–18 GHz was covered with a logarithmic sweep over 1601 frequency points, *i.e.* the frequencies measured had a logarithmic distribution over the range.

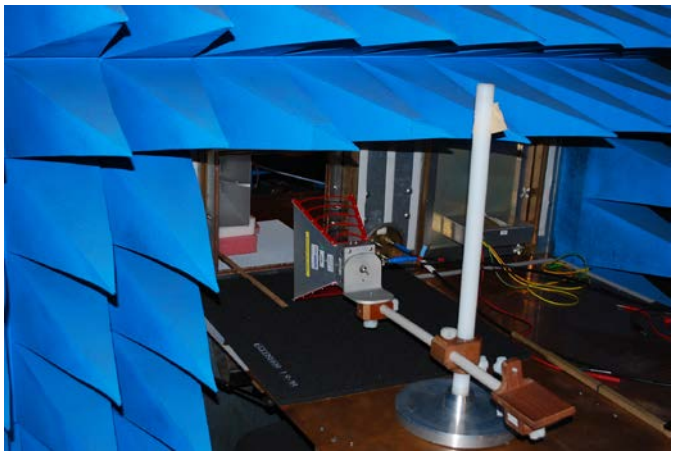

Fig. 2. Photo showing the set-up from inside the SAC.

B. Determination of Aperture Transmission Cross Section and Shielding Effectiveness in Reverberation Chamber

The shielding properties of the glass structures were also measured at isotropic conditions in a RC, see Fig. 3 and Fig. 4. An isotropic environment yields an average value of the transmission of plane waves incident on the test object from (ideally) all directions and with (ideally) all polarizations. In this case the shielding properties are expressed in terms of the isotropic transmission cross section, $\langle\sigma_a\rangle$, of the glass structure (where the brackets indicate that the cross section has been measured at isotropic conditions). At plane wave conditions the transmission cross section, σ_a, of an aperture has the following definition [10]:

$$P_{trans} = \sigma_a(\theta,\phi,p)\cdot S_{inc}(\theta,\phi,p). \tag{2}$$

In (2) P_{trans} is the power transmitted through the aperture. The parameters θ and ϕ denote the angle of incidence of the plane wave and p its polarization. S_{inc} is the power density of the incident field.

In an isotropic environment one gets:

$$P_{trans} = \langle\sigma_a\rangle \cdot S_{sc,Rev} \tag{3}$$

where $\langle\sigma_a\rangle$ is achieved by averaging σ_a over all angles and polarizations and $S_{sc,Rev}$ is the so called scalar power density in the reverberation chamber. The concept of scalar power density was introduced by Hill [11].

The rationale behind choosing the transmission cross section is that it consists of an absolute result, given in square meters, of the shielding properties of the structure. As is shown in *e.g.* [10] the outcome of a measurement of σ_a (or $\langle\sigma_a\rangle$ in case of an isotropic external environment) can be used to calculate the average shielding effectiveness $\langle SE\rangle$ of an overmoded cavity (denoted by index *cav*) backing the aperture by:

$$\langle SE\rangle = \frac{S_{inc}}{S_{sc,cav}} = \frac{2\pi\cdot V}{\sigma_a\cdot\lambda\cdot Q}. \tag{4}$$

In (4) V is the cavity volume, λ the wavelength and Q the cavity quality factor. $S_{sc,cav}$ is the scalar power density of the field inside the cavity. The average, denoted by the brackets, is taken over uncorrelated field points over the entire internal volume of the cavity.

Equation (4) highlights the important fact that shielding effectiveness for an overmoded cavity does not only depend on the properties of the apertures causing the leakage into the cavity but also on the volume and Q-value of the cavity (and of the wavelength).

In our measurements $\langle\sigma_a\rangle$ is determined by relating P_{trans} for the aperture under test (AUT) with P_{trans} for a 30 mm diameter circular aperture, based on an analytical solution of σ_a for a circular aperture, *cf.* [11]. $\langle\sigma_a\rangle$ can also be derived by use of (4) provided Q has been determined for the nested cavity.

The method assumes that the cavity Q-value does not change dramatically between the reference measurement and AUT measurement. In the present case this implies that $\langle \sigma_a \rangle$ for the AUT shall not exceed -32 dBm^2, *i.e.* that $\langle SE \rangle$ must be greater than 15 dB in order to have a measurement error less than 1 dB.

1) Isotropic transmission cross section expressed in terms of shielding effectiveness

In the present case the reference aperture is a square opening with an area *A*, 300 x 300 mm^2. For a reference aperture with such a simple geometry one may express the result above in terms of shielding effectiveness, *i.e.* in terms of a dimensionless quantity, simply by comparing the power transmitted through the unshielded opening (*i.e.* the square opening) with the power transmitted through the opening when the shielded structure is mounted on it, *i.e.*

$$\langle SE_{apert,iso} \rangle = \frac{A/4}{\langle \sigma_a \rangle}. \quad (5)$$

The reason for dividing the area of the open square aperture by 4 is due to the isotropic conditions in the RC; since this implies that the transmission cross section of an electrically large aperture is equal to *A*/4 [10], [11]. One factor of two comes from the fact the irradiation strikes the aperture not only at normal incidence but also at slant angles, yielding a cosine dependence of the transmitted power [11], and an additional factor of two due to the fact that the aperture is irradiated from a half sphere while the field in the RC is defined and measured far away from the walls.

In (5) we approximate the transmission cross section of the unshielded opening by *A*/4 which is exactly true only at frequencies where the opening is electrically large. For frequencies above 1 GHz the error is less than 1 dB.

2) Measurement set-up

Inside the RC a smaller cavity (nicknamed 'Akilles') (size 1.53 x 0.93 x 0.69 m^3) is nested via a square aperture sized 300 mm by 300 mm, Fig. 3 and Fig. 4. Mode stirrers are located inside both chamber and cavity to generate different field conditions by altering the boundary conditions. The RC stirrer is rotated in 21 positions and for each position the internal stirrer inside the cavity steps through 12 positions, in combination totaling 252 positions. The measured field inside the cavity can thus be considered uncorrelated and hence the

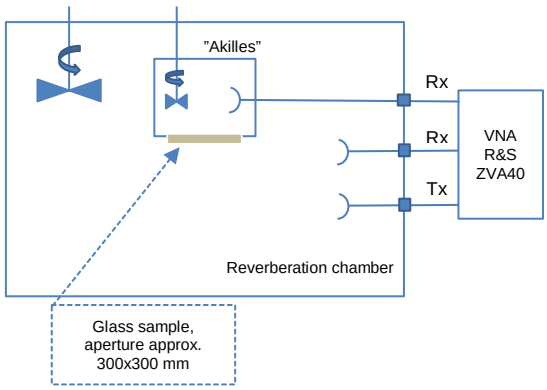

Fig. 3 Simplified block diagram showing the reverberation chamber

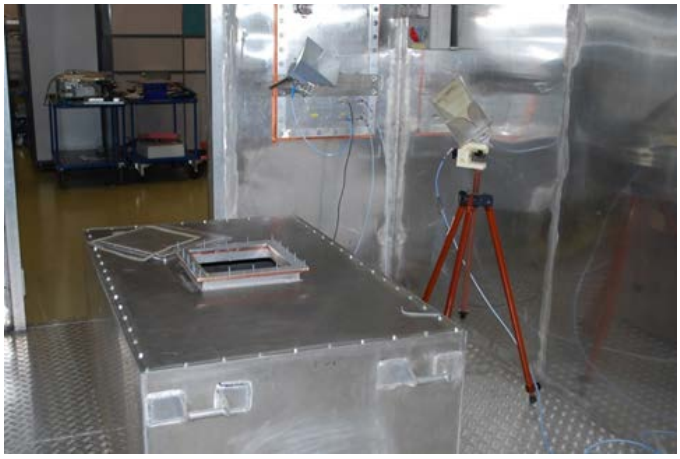

Fig. 4. The internal cavity "Akilles" inside the reverberation chamber.

$\langle SE \rangle$ measured using an average of the measured field for all positions, per frequency, as described above.

III. Measurement Samples

The samples are divided in two groups; single window panes, and complete window units without sash and frame.

The first group, single window panes, is tabulated in Table I. The code found in the first column is an identifier for each specimen; the second column tells of what specific type the specimen is and the two last columns show how many of the samples were tested in the RC and the SAC respectively.

Clear glass panes are included as reference samples. However, they cannot be measured in the RC due to the low RF attenuation. Soft coated and hard coated low-emission glass are intended to reflect infrared light (i.e. heat) back while letting day-light pass through them. The difference between the two is the composition and method used for deposition of the coating layer.

Soft coating is deposited on float glass in tens of nanometers thick layers using physical vapor deposition (PVD) where the layers consist of various metal oxides, typically tin-dioxide (SnO_2) interleaved with one or more layers of silver. Other metal oxides such as ZnO and TiO_3 may also be used. Soft coated windows are also commonly referred to as solar control windows due to the reflection of the high-energy ultra-violet rays of the sunlight which otherwise, when hitting objects behind the window would generate heat. The more layers the lower emissivity and the better the reflection of ultra-violet light.

Hard coating is applied using chemical vapor deposition (CVD) in the production line, on semi-molten glass, yielding only one, a few hundreds of nm thick, layer of SnO_2.

A spandrel pane is an opaque glass often placed as cladding element between clear-view windows in all-glass façades to cover construction elements, insulation and building infrastructure installations. The opacity is achieved by adding coatings of metal, metal oxides or enamel on the rear (inner) side of the pane.

TABLE I.
MEASUREMENT SAMPLES – SINGLE WINDOW PANES AND THE NUMBER OF SAMPLES RUN IN RC AND SAC RESPECTIVELY

Single Panes, Standard Types			
Specimen No	***Specimen type***	***No of Samples in RC***	***No of Samples in SAC***
CG-1 – CG-3	Clear Glass (Float Glass)	-	3
Sp-1 – Sp-5	Spandrel Glass	1	5
HC-1 – HC-5	'Hard Coated' Low-emission Glass	1	5
1Ag-1 – 1Ag-5	'Soft Coated' Glass 1 Silver Layer	1	5
2Ag-1 – 2Ag-5	'Soft Coated' Glass 2 Silver Layers	1	5

The development of energy saving windows has taken a number of distinct steps over time, from detachable windows via windows with coupled sash to energy saving windows with double-glazed sash with clear glass and dry air in between the panes, using the vacuum-flask principle. From there triple-glazed energy saving windows developed and the next generations include coated low-emission panes to further improve the energy saving functionality. In Table II four generations of energy saving windows are listed where the W2I and W3I types mostly were installed during the 1970's and 1980's. The W3LE type began to gain popularity in the 1990's and W3UL can be considered state of the art today in the 2010's. The window samples of the four generations can be seen in Fig. 5. Note the copper tape which was applied around the edge of the two rightmost windows during the tests.

TABLE II.
MEASUREMENT SAMPLES – COMPLETE WINDOW UNITS (WITHOUT SASH) AND THE NUMBER OF SAMPLES RUN IN RC AND SAC RESPECTIVELY.

Window Units			
Specimen No	***Specimen type***	***No of Samples in RC***	***No of Samples in SAC***
W2I	Double-glazed Energy saving window	-	1
W3I	Triple-glazed Energy saving window	-	1
W3LE	Triple-glazed Low-emission window	1	1
W3UL	Triple-glazed Ultra-low e-glass	1	1

IV. RESULTS

Here we will present the measurement results for A – complete window units, B – single window panes, and at the end, C – discuss some observations.

A. Window Units

The first measurements were of $\langle \sigma_a \rangle$ in the reverberation chamber. As shown in (5) $\langle SE \rangle$ can be obtained using the measured $\langle \sigma_a \rangle$ while *SE* according to (1) is measured in the semi-anechoic chamber at only one angle of incidence. Although the methods and environments are quite different we expect the resulting traces to exhibit a similar behavior over frequency. However, the $\langle SE \rangle$ trace from the RC can be expected to exhibit a smoother shape due to the isotropic conditions under which it is captured. On the other hand, the *SE* (plane wave) trace should suffer from more rapid variations due to resonances that are depending of the aperture size and shape

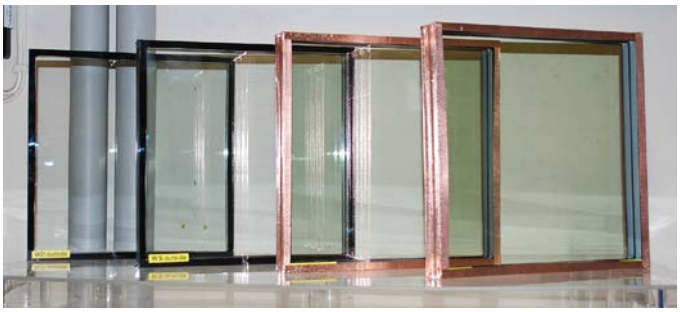

Fig. 5. The four window types used in the measurements. From left to right: W2I, W3I, W3LE and W3UL.

Comparing the $\langle SE \rangle$ traces seen in Fig. 6 with the *SE* traces in Fig. 7 clearly points out the difference between the two methods. *E.g.* the upper (red) trace in Fig. 6 corresponds to the upper trace in Fig. 7 it is possible to see that the trends resemble. The same thing can be said about the second trace from top in both figures (blue) where the trends follow each other. The attenuation through W2I and W3I is too low to for isotropic measurements and is hence not measured in RC (thus not presented in Fig. 6).

The results as seen in Fig. 7 show that there is a clear generation gap *SE*-wise between "energy saving" windows (W2I and W3I) and "low-emission" windows (W3LE and W3UL). The first basically exhibit no RF attenuation at all, except in the 4-6 GHz range and between approximately 11 and 14 GHz where the shielding effectiveness rises from almost zero to around 10 dB. The latter shows $\langle SE \rangle$ numbers spanning from 10 to over 45 dB where the more modern W3UL largely outperforms the W3LE at the highest and lowest frequencies.

When measuring the window units in the reverberation chamber it was discovered that the low-emission windows required copper taping on the sides. For a further discussion on this see section IV.C.

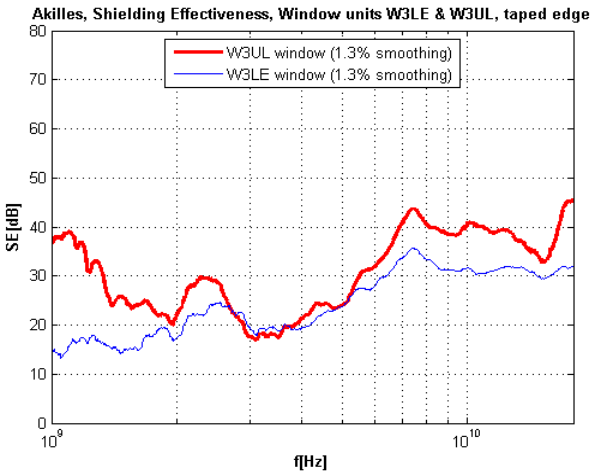

Fig. 6. Results comparing the isotropic measurements of sheilding effectiveness, $\langle SE \rangle$, in the RC, for W3LE, and W3UL windows.

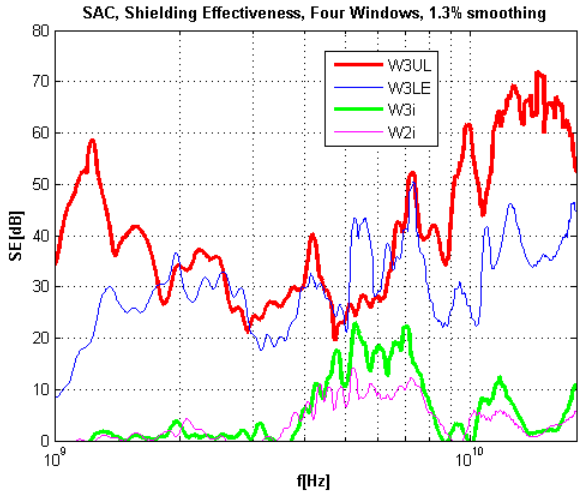

Fig. 7. Results comparing the plane wave measurements of shielding effectiveness, SE, in the SAC for W2I, W3I, W3LE, and W3UL windows.

B. *Window Panes*

Since the attenuation through clear glass (CG) is too low to conduct isotropic measurements it was not measured in the RC and is hence not available in Fig. 8.

When comparing the two kinds of measurements in Fig. 8 and Fig. 9 the general trends are similar with the exception of the double layer silver coated glass, 2Ag. The reason for this deviation is yet to be explained.

Again we can observe the difference in fine structure between the two methods, presumably depending on side leakage enabling resonances within the glass or between conductive surfaces.

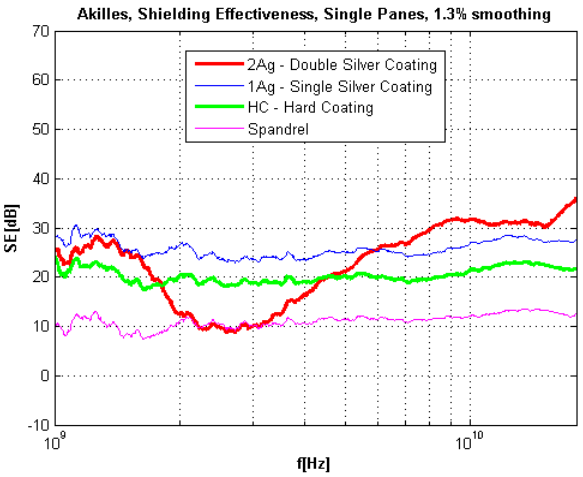

Fig. 8. Results comparing the isotropic measurements of sheilding effectiveness, ⟨SE⟩, i in the RC, for 1Ag, 2Ag, SC, and HC panes. Notable is the trace from the double-silver pane that deviates substantially from the shape of the other three.

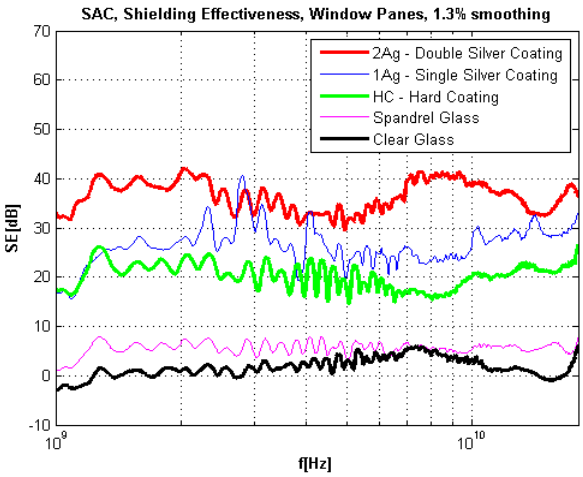

Fig. 9. Results comparing the plane wave measurements of sheilding effectiveness, *SE*, in the SAC, for CG, SC, HC, 1Ag, and 2Ag panes.

C. *Observations*

When measuring the window units in the reverberation chamber it was discovered that when placing a metal cover over the aperture there was no noticeable increase of $\langle SE \rangle$ *cf.* Fig. 10, the two lower traces in magenta and green. Copper tape applied around the edges of the units resulted in an increased $\langle SE \rangle$ from 5 GHz and upwards according to the blue trace.

As a final test to verify the efficiency of the tape the metal cover was applied again, see the red, upper trace in Fig. 10. Here a substantial increase in $\langle SE \rangle$ was achieved between 1 and 7 GHz while the trace above 7 GHz completely coincides with the blue trace which is measured without the metal plate covering the aperture.

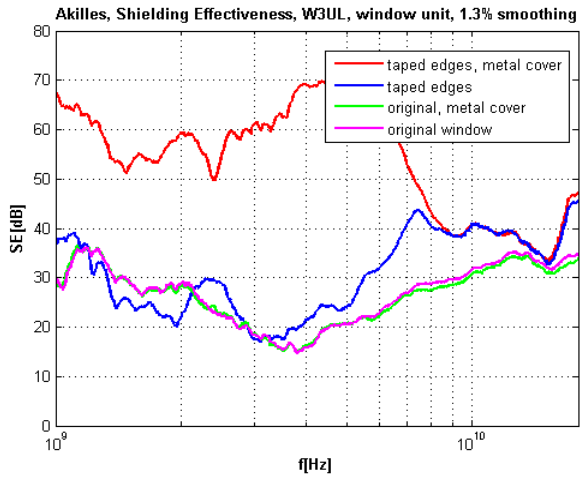

Fig. 10. Results comparing the isotropic measurements of ⟨SE⟩ in the RC, for W3UL windows. The lower two trace (overlapping) shows the W3UL window w. and w.o. metal cover. The upper two traces shows the same window with edges covered w. copper tape.

V. Conclusions

Measurement results have been presented for a group of window panes intended for different window applications and for a group of window units representing four different generations. Both groups have been measured under isotropic conditions in a nested reverberation chamber to yield the $\langle SE \rangle$ through the isotropic transmission cross section, $\langle \sigma_a \rangle$, and in a semi-anechoic chamber under plane wave conditions yielding the shielding effectiveness, *SE*.

The *SE* from a comparative measurement in an SAC as described in this paper should equal $(A/4)/\sigma_a$ if the *SE* dependence of angle of incidence and polarization is equal for "hatch on" and "hatch off"; and if the radiation pattern behind the AUT is identical to the reference opening ("hatch off"). However we could show that this is strictly not the case since there will be side leakage creating fringed radiation patterns where the result of the *SE* measurement is highly dependent of the receiver antenna position. Suffice a very small shift in position sideways to have a major change in the *SE*.

During the study of the low-emission windows in the RC we found that there is a strong side-leakage meaning that the windows must be mounted in window sashes of metal, rather than of wood as is common in the Swedish construction tradition.

In this study we have shown that different types of coated window panes exhibit great differences in RF attenuation from approximately 10 dB to 30 dB, over the 1 – 18 GHz range, as compared to almost 0 dB for traditional clear float glass. We have also shown that modern low-emission window structures attenuate the signal frequency dependent by 15 – 45 dB over the same frequency range. Both the Low-e (W3LE) and the Ultra-Low-e (W3UL) shows a peak in *SE* at 2 – 3 GHz and a high plateau when reaching above 7 GHz. This implies that apart from energy-saving, IEMI qualifies among the reasons to upgrade the windows of a vulnerable building.

We have also shown that measuring isotropic transmission cross section, $\langle \sigma_a \rangle$, under isotropic conditions in a nested reverberation chamber can reveal issues, *i.e.* side leakage, that are impossible to detect immediately when measuring the shielding effectiveness, *SE*, with plane wave measurements at normal incidence.

Further analysis will be made using numerical simulations on glass structures.

Acknowledgments

This work is a part of the project *Protection against Electromagnetic Risks. Intentional Electromagnetic Interference (IEMI)*, funded by the Swedish Civil Contingencies Agency (MSB), the Swedish Fortifications Agency, The Swedish Post and Telecom Authority (PTS) and The National Food Agency (SLV). The authors also wish to emphasize the support from Mikael Ludvigsson and Maria Lang at the Swedish Glass Research Institute, Glafo, who were very helpful in the selection and acquisition of test samples.

References

[1] W. A. Radasky and M. Bäckström, "Brief historical review and bibliography for Intentional Electromagnetic Interference (IEMI)," in *General Assembly and Scientific Symposium (URSI GASS), 2014 XXXIth URSI*, Beijing, China, 16-23 Aug. 2014.

[2] W. A. Radasky, C. E. Baum and M. W. Wik, "Introduction to the Special Issue on High-Power Electromagnetics (HPEM) and Intentional Electromagnetic Interference (IEMI)," *IEEE Trans. Electromagn. Compat.*, vol. 46, no. 3, pp. 314-321, 2004.

[3] F. Sabath, "What can be learned from documented Intentional Electromagnetic Interference (IEMI) attacks?," in *General Assembly and Scientific Symposium, 2011 XXXth URSI*, Istanbul, Turkey, 13-20 Aug. 2011.

[4] S. van de Beek and F. Leferink, "Current Intentional EMI studies in Europe with a Focus on STRUCTURES," in *Electromagnetic Compatibility, Tokyo (EMC'14/Tokyo), 2014 International Symposium on*, Tokyo, Japan, 2014.

[5] E. Krogager and J. Godø, "Attenuation of Building used for HPM Testing," in *AMEREM-2014*, Albuquerque, NM, USA, 2014.

[6] A. Asp, Y. Sydorov, M. Valkama and J. Niemelä, "Radio Signal Propagation and Attenuation Measurements for Modern Residential Buildings," in *Globecom Workshops (GC Wkshps), 2012 IEEE*, Anaheim, CA, USA, 2012.

[7] I. Rodriguez, H. C. Nguyen, N. T. Jorgensen, T. B. Sorensen and P. Mogensen, "Radio Propagation into Modern Buildings: Attenuation Measurements in the Range from 800 MHz to 18 GHz," in *Vehicular Technology Conference (VTC Fall), 2014 IEEE 80th*, Vancouver, Canada, 2014.

[8] G. I. Kiani, A. Karlsson, L. Olsson and K. P. Esselle, "Glass Characterization for Designing Frequency Selective Surfaces to Improve Transmission through Energy Saving Glass Windows," in *Microwave Conference, 2007. APMC 2007. Asia-Pacific*, Bangkok, Thailand, 2007.

[9] P. Ragulis, Ž. Kancleris and R. Simniškis, "Transmission and Reflection of Microwave Radioation from Novel Window Panes," in *AMEREM-2014*, Albuquerque, NM, USA, 2014.

[10] M. Bäckström, T. Nilsson and B. Vallhagen, "Guideline for HPM protection and verification based on the method of power balance," in *Electromagnetic Compatibility (EMC Europe), 2014 International Symposium on*, Gothenburg, Sweden, 2014.

[11] D. A. Hill, M. T. Ma, A. R. Ondrejka, B. F. Riddle, M. L. Crawford and R. T. Johnk, "Aperture Excitation of Electrically Large, Lossy Cavities," *IEEE Trans. Electromagn. Compat.*, vol. 36, no. 3, pp. 169-178, August 1994.